

CYLINDRICAL CAVITY DESIGN AND PARTICLE-TRACKING SIMULATION IN CYCLOTRON AUTO-RESONANCE ACCELERATOR*

Yating Yuan, Kuanjun Fan[†], State Key Laboratory of Advanced Electromagnetic and Technology, Huazhong University of Science and Technology, [430074] Wuhan, China
Yong Jiang[‡], Yale University, [06520] New Haven, USA

Abstract

The Cyclotron Auto-Resonance Accelerator (CARA) is a novel concept of accelerating continuous-wave (CW) charged-particle beams. This type of accelerator has applications in environment improvement area and generation of high-power microwaves. In CARA, the CW electron beam follows a gyrating trajectory while undergoing the interaction with a rotating TE₁₁-mode RF field and tapered static magnetic field. The cylindrical cavity operating at TE_{11p}-mode is adapted to accelerate electron beam. The cavity size is optimized to obtain a beam with designed energy, then a design method of the TE_{11p}-mode acceleration cavity is described here. Moreover, regardless of space charge effect, several particle-tracking simulations of CARAs are showed.

INTRODUCTION

Researches and experiments have been implemented to study the concept underlying Cyclotron Auto-Resonance Accelerator (CARA) over the past 50-years [1-5], wherein gyrating electron beam is maintained in phase synchronism with a rotating TE11-mode waveguide RF field using tapers in magnetic field or waveguide radius. CARA has many unique features, including remarkably high RF-to-beam efficiency (measured at >96%) [3], generation of a continuous self-scanning beam (without bunching and external scanning structures), simple one-stage cylindrical accelerating structure [6] and lower beam loading on output window, as compared with the typical linear accelerator. It has many applications in environment improvement area and generation of high-power microwaves [7]. Two concepts described here based and go beyond prior work, namely (a) design method of a TE_{11p} cylindrical cavity for CARA; and (b) several particle-tracking simulations of CARAs under different RF power frequency.

THEORETICAL ANALYSIS

Gyroresonant Acceleration Theory

In CARA, the electron beam follows a gyrating trajectory under the rotating TE₁₁-mode waveguide field and axial static magnetic field [1, 3, 5]. The TE₁₁-mode field only has transverse E-field, which can be used to accelerate electron transversely as shown in Fig. 1. The blue arrow represents the transverse E-field on the cross section; the red point is the electron; and the red circle represents the cyclotron motion of the electron. When the direction of E-

field is parallel (180 degree) to the tangential velocity of the electron, the electron will get accelerated most effective. At resonance, the electron gyrates with the rotating electric field at the same cyclotron frequency, then the electron will be accelerated at any time as displayed in Fig. 1. The continuously accelerating is achieved, named “RF gyroresonant acceleration”.

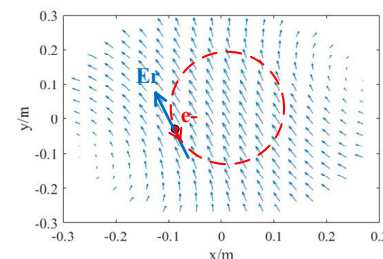


Figure 1: TE₁₁ E-field and electron on cross section.

In the presence of the axial magnetic field $B_0(z)$, the particle executes an additional cyclotron motion. The cyclotron frequency of particles of charge e and rest mass m_0 in consideration of relativistic factor γ is $\Omega = eB_0(z)/m_0\gamma$. The frequency of RF wave seen by the particle (in the laboratory frame) is $\omega - k_z c \beta_z$ where ω is the frequency of RF source, k_z is the wave number in z direction, c is the light speed and β_z is the normalized axial velocity of particle. If these two frequencies are made to coincide, one expects some resonance effect to occur in the particle motion. So the resonance condition [7] is $\omega - k_z c \beta_z - \Omega = 0$ or $b_0 = \gamma(1 - n\beta_z)$, where $n = k_z c / \omega$ is the effective refractive index for the operating mode. The synchronous B-field is $B_0(z) = \frac{m_0 \omega \gamma}{e} (1 - n\beta_z)$. $B_0(z)$ is related to the energy and velocity of particle, which are varying with time and are affected by the magnetic field at last position. In this paper, adapting multiple iterations to obtain $B_0(z)$.

The maximum energy can be reached using an up-tapered B-field, until mirror-reflection leads to stalling [6, 7]. The maximum accelerated energy is given approximated by $\gamma_{\max} = \gamma_0 + \left(\frac{\gamma_0^2 - 1}{1 - n_1^2} \right)^{1/2}$, where n_1 is the refractive index at the end of CARA, γ_0 is the initial value of the particle energy factor. Practical implications of the limit are illustrated in Fig. 2: the larger n_1 and γ_0 of particle, the

* Work supported by the National Natural Science Foundation of China

† kjfan@hust.edu.cn

‡ yong.jiang@yale.edu

larger the energy limit γ_{\max} ; and n_1 required to close to unity to get large γ_{\max} .

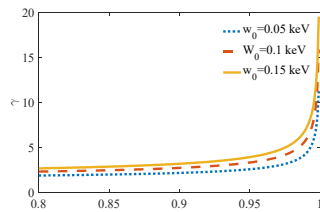


Figure 2: Energy limit in CARA plotted as the refractive index n approaches unity for several particle injection energy.

Design of TE_{11p} -Mode Cavity in CARA

The CARA can be achieved both in a cylindrical waveguide or cavity. It is suggested to employ standing-wave cavity comparing with traveling-wave waveguide in order to avoid the size and complexity of the resonant ring. Besides, the standing-wave cavity can offer comparable RF-to-beam efficiencies and wall losses are similar when the extra length of the resonant ring is taken into account [7]. This paper adapts TE_{11p} cylindrical cavity. And the up-tapered B-field is used to achieve the resonance condition.

For TE_{11p} -mode in cylindrical cavity, defining axial field cycle length is l_1 and the radius is r , so the total length of the cavity is $l = l_1 p$. Then the refractive index of TE_{11p} -mode is $n = 1 / \sqrt{(1.841 \cdot l_1 / r \cdot \pi)^2 + 1}$ and the resonant frequency is $f = \frac{c}{2\pi} \cdot \sqrt{(1.841/r)^2 + (\pi/l_1)^2}$, which indicates the refractive index and resonant frequency are both only related to l_1 and r for TE_{11p} -mode in cylindrical cavity. Supposing the injection energy of electron beam is 0.1 MeV, the refractive index n , resonant frequency f and energy limit γ_{\max} at different cavity size l_1 and r are shown

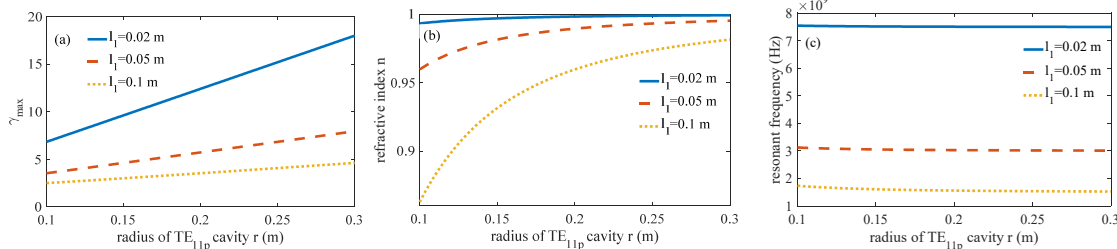


Figure 3: Dependence of (a) energy limit γ_{\max} ; (b) refractive index n ; and (c) resonant frequency f on cavity radius r for different axial cycle length l_1 .

NUMERICAL PARTICLE-TRACKING SIMULATIONS

The peak E-field in the cavity is fixed at 2 MV/m. The injection and target output energy are 0.1 MeV and \sim 2 MeV respectively. The cylindrical cavity is designed according to the above steps when the RF power frequency is 1.3, 2.856, and 5.712 GHz, respectively. Supposing the injection electron beam has only axial velocity, and particle-tracking simulation is performed regardless of the space

in Fig. 3. γ_{\max} is almost linear with r ; large n can be achieved at large r and small l_1 ; and r has little effect on f while l_1 has great influence under the change scale of r and l_1 . And the smaller the RF power frequency is, the larger l_1 is. Then the required r is larger in order to get large γ_{\max} . Given the frequency of RF power f , the beam injection energy W_0 and the required output energy W_1 , then the cavity size r and l_1 can be designed:

(a) The range of the radius r can be calculated from the cut-off frequency of TE_{11p} -mode: $r \geq 1.841 \cdot c / 2\pi f$.

(b) f is almost affected by l_1 , so the approximate range of l_1 can be determined by f (the r value is arbitrarily given 0.2):

$$l_1 = \pi / \sqrt{(2\pi f / c)^2 + (1.841/r)^2} \text{ and } l_1 > c / 2f.$$

(c) The minimum value of required refractive index n can be derived from the input and output energy of particle

$$\text{by the } \gamma_{\max} \text{ formula: } n = \sqrt{1 - \frac{\gamma_0^2 - 1}{(\gamma_{\max} - \gamma_0)^2}}.$$

(d) The value of r can be obtained from the formula of n after n and l_1 are determined: $r = 1.841 \cdot l_1 / \sqrt{\frac{1-n^2}{n^2}} \cdot \pi$.

(e) The f formula is used to correct r and l_1 : if f is too large, then correct r (increase r); or if f is too small, then correct l_1 (decrease l_1). Because increasing r or decreasing l_1 can both increase n .

$$l_{1_correct} = \pi / \sqrt{(2\pi f / c)^2 - (1.841/r)^2}$$

$$r_{correct} = 1.841 / \sqrt{(2\pi f / c)^2 - (\pi / l_1)^2}$$

After determining the cavity size r and l_1 , the guided axial B-field, RF field strength and axial cycle number p are required to optimize to realize the resonance condition between the RF field and electron beam.

charge effect. Table 1 lists computed parameters for several 1.3, 2.856, 5.712 GHz, \sim 2 MeV CARAs. The corresponding simulation results of the electron cyclotron frequency, gyro radius, γ , axial velocity V_z , transverse velocity V_T and the optimized guided axial B-field are shown in Fig. 4. The beam trajectory is shown in Fig. 5.

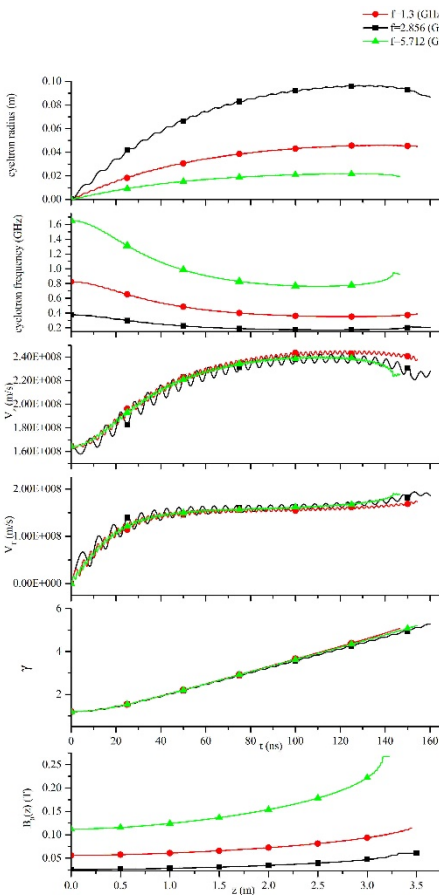


Figure 4: Dependence of cyclotron radius, cyclotron frequency, γ , axial velocity V_z and transverse velocity V_T on time t and the optimized guided axial B-field on z .

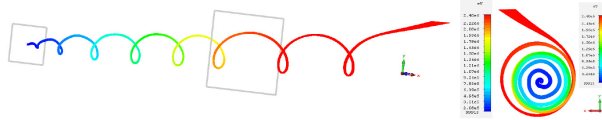


Figure 5: The electron beam trajectory in CARA.

Table 1: Parameters for Several 1.3, 2.856, 5.712 GHz, ~2 MeV CARAs

	Case 1	Case 2	Case 3
Driven Frequency (GHz)	1.3	2.856	5.712
Cavity Radius r (cm)	39.26	19.63	8.83
Cycle Length l_1 (cm)	11.71	5.31	2.66
Refractive Index n	0.9851	0.9876	0.9874
γ_{\max} (theoretical)	5	5.3	4.96
Axial Cycle Numbers p	30	65	121
Total Length (m)	3.51	3.45	3.22
γ_{out}	5.26	5.2	5
Wall loss (W)	5.09e5	6.66e5	8.16e5

Table 1 indicates: Under the same electron injection and output energy, r and l_1 need to be smaller with the higher RF power frequency. In order to get ~2 MeV output beam,

the total cavity length l at three different RF source frequencies are almost the same when the peak E-field is fixed. The axial cycle numbers p and wall loss P_c increases with RF source frequency.

From the results in Fig. 4, the law of electron beam parameters during acceleration can be obtained:

- The axial synchronous B-field gradually increases along z direction with the slope becomes larger and larger;
- The cyclotron frequency of electron gradually decreases while cyclotron radius gradually increases;
- The γ value increases approximately linearly;
- V_z and V_T both increase and V_T increases more than V_z .

The axial B-field and cyclotron frequency increase while gyration radius falls with RF power frequency. However, the γ and velocity of electron change with time at different RF power frequency are similar. Numerical simulations show a slight energy excess above the theoretical prediction when an optimized B-field is introduced. Since the peak E-field in the cavity is fixed, and the electron beam is accelerated by the tangential force of the transverse RF E-field, as shown in Fig. 1, the cyclotron motion circumstance of the electron directly affects the energy increment. The circumstance is proportional to the cyclotron radius and frequency. Although the cyclotron frequency increases with the RF power frequency, the cyclotron radius decreases. So there is not much different in total cavity length at different RF power frequency. From the energy limit formula, the large cavity radius r can reach large output electron energy, however, this strategy has limited utility, since for a fixed RF power level, the accelerating gradient drops as r increases, thus lengthening the structure and thereby limiting its practical utility. A standing-wave is the superposition of two counter-propagating travelling waves. In fact, electron interacts only with the traveling wave propagating in the positive z direction while detunes with the other one, which will destroy the electron stability during acceleration. Therefore, it can be seen that there is a certain oscillation in the gamma and velocity curves, and the higher the RF power frequency, the larger the oscillation frequency and the amplitude.

CONCLUSIONS

The design process of TE_{11p}-mode cylindrical cavity in CARA has been established. And several 1.3, 2.856, 5.712 GHz, ~2 MeV CARAs have been designed and simulated, from which the effect of cavity size on CARA performance, the electron beam motion during acceleration are analysed. The CARA competitive edge arises from (a) a simpler and cheaper geometry of the accelerator structure; (b) the continuous accelerating process with high RF-to-beam efficiency; (c) the self-scanning output beam without external device. However, the ungainly-sized structure exposes a possible disadvantage of CARA.

REFERENCES

- [1] B. Hafizi, P. Sprangle, and J. L. Hirshfield, “Electron beam quality in a cyclotron autoresonance accelerator”, *Phy. Rev. E.*, vol. 50, pp. 3077-3086, 1994. doi: [10.1103/PhysRevE.50.3077](https://doi.org/10.1103/PhysRevE.50.3077)
- [2] D. B. McDermott, D. S. Furuno, and N. C. Luhmann Jr, “Production of relativistic, rotating electron beams by gyroresonant rf acceleration in a TE₁₁₁ cavity”, *Journal of Applied Physics*, vol. 58, pp. 4501-4508, 1985. doi: [10.1063/1.336262](https://doi.org/10.1063/1.336262)
- [3] M. A. LaPointe, R. B. Yoder, Changbiao Wang, A. K. Ganguly, and J. L. Hirshfield, “Experimental Demonstration of High Efficiency Electron Cyclotron Autoresonance Acceleration”, *Phy. Rev. Lett.*, vol. 76, pp. 2718-2721, 1996. doi: [10.1103/PhysRevLett.76.2718](https://doi.org/10.1103/PhysRevLett.76.2718)
- [4] J. L. Hirshfield, M. A. LaPointe, A. K. Ganguly, R. B. Yoder, and Changbiao Wang, “Multimegawatt cyclotron autoresonance accelerator”, *Physics of Plasmas*, vol. 3, pp. 2163-2168, 1996. doi: [10.1063/1.871670](https://doi.org/10.1063/1.871670)
- [5] Yating Yuan, Kuanjun Fan, and Yong Jiang, “Dynamic behaviour of electron beam under rf field and static magnetic field in cyclotron auto resonance accelerator”, in *Proc. 29th Linear Accelerator Conf. (LINAC'18)*, Beijing, China, Sep. 2018, pp. 725-728. doi: [10.18429/JACoW-LINAC2018-THP0020](https://doi.org/10.18429/JACoW-LINAC2018-THP0020)
- [6] Yong Jiang, Sergey V. Shchelkunov, and Jay L. Hirshfield, “Cyclotron Auto-Resonance Accelerator for environmental applications”, in *Proc. AIP Conference*, Mar. 2017, pp. 060003-1-060003-5. doi: [10.1063/1.4975870](https://doi.org/10.1063/1.4975870)
- [7] J. L. Hirshfield and Changbiao Wang, “Energy limit in cyclotron autoresonance acceleration”, *Phy. Rev. E.*, vol. 51, pp. 2456-2464, 1995. doi: [10.1103/PhysRevE.51.2456](https://doi.org/10.1103/PhysRevE.51.2456)